Mirabilin, an Antitumor Macrolide Lactam from the Marine Sponge *Siliquariaspongia mirabilis*†

Alberto Plaza, Heather L. Baker, and Carole A. Bewley*

Laboratory of Bioorganic Chemistry, National Institute of Diabetes and Digestive and Kidney Diseases, National Institutes of Health, Bethesda, Maryland 20892-0820

Received October 27, 2007

A new highly unsaturated macrolide lactam, termed mirabilin (**1**), was isolated from the aqueous extract of the marine sponge *Siliquariaspongia mirabilis*. Mirabilin is characterized by the presence of a 35-membered macrolide lactam ring bearing a pentadiene conjugated system and a tetrasubstituted tetrahydropyran ring. A linear polyketide moiety is attached to the macrocyclic ring through an amide linkage. The structure of mirabilin was determined using extensive 2D NMR and ESIMS and tandem MS techniques. Mirabilin inhibits the growth of the tumor cell line HCT-116 with an IC_{50} value of 0.27 ± 0.09 μM and is noncytotoxic to several other cell lines.

Lithistid demosponges have proven to be among the richest sources of structurally diverse marine natural products.[1] Sponges belonging to the family Theonellidae in particular have yielded a number of novel macrolides exhibiting remarkable biological activities. A few examples include the potent cancer cell growth inhibitors swinholides,[2a–g] bistheonellides A and B,[3] sphinxolides,[4] superstolides,[5] and recently reported hurghadolide.[2g] In our continuing efforts to identify new bioactive natural products from marine organisms, we have been studying the extracts of the lithistid demosponge *Siliquariaspongia mirabilis* collected from the archipelago of Chuuk. Recently we reported the structures of several new anti-HIV glycosidated depsipeptides, mirabamides A−D,[6] that we purified from the aqueous extract of *S. mirabilis*. Further screening against a human colon carcinoma cell line (HCT-116) showed that this same aqueous extract inhibited tumor cell growth at 50 μg/mL. Bioassay-guided separation of the cytotoxic extract led to the isolation of a highly unsaturated macrolide lactam, termed mirabilin (**1**), which was responsible for the activity of the aqueous extract. Its structure was elucidated by extensive analysis of NMR data, including 1D (^{1}H and ^{13}C) and 2D homonuclear and heteronuclear NMR experiments (DQF-COSY, HOHAHA, HMBC, HSQC, HSQC-TOCSY, and ROESY), as well as ESIMS and tandem MS data.

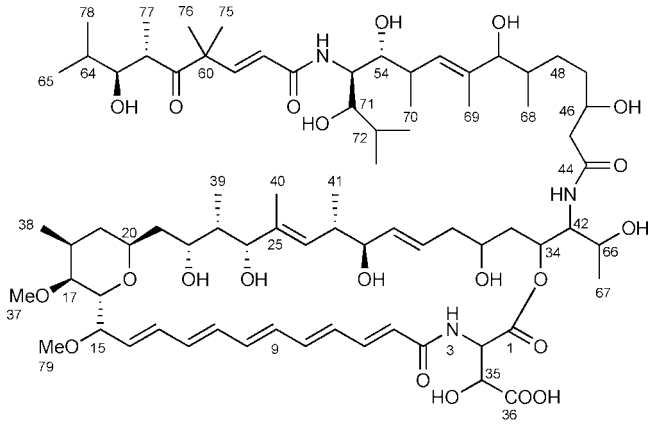

1

The aqueous extract of *S. mirabilis* was partitioned between *n*-BuOH and H_2O. Chromatography of the *n*-BuOH extract over Sephadex LH-20 followed by reversed-phase HPLC yielded compound **1**. The molecular formula of **1** was established as $C_{76}H_{123}N_3O_{22}$ on the basis of HRESIMS (*m/z* 1428.8442 $[M - H]^-$, calcd for $C_{76}H_{122}N_3O_{22}$, 1428.8520) and NMR spectral data (see Table 1). The IR spectrum of **1** displayed absorption bands at 3380 and 1680 cm^{-1}, indicating the presence of hydroxyl and ester functionalities, while a UV absorption band at 350 nm and the yellow color of the pure compound suggested the presence of a conjugated polyene moiety. The ^{1}H NMR spectrum of **1** contained signals for 11 methyl doublets at δ 0.54 (3H, d, J = 7.0 Hz), 0.68 (3H, d, J = 6.7 Hz), 0.87 (3H, d, J = 6.9 Hz), 0.92 (3H, d, J = 6.8 Hz), 0.95 (3H, d, J = 6.6 Hz), 0.988 (3H, d, J = 6.9 Hz), 0.99 (3H, d, J = 6.5 Hz), 1.02 (3H, d, J = 6.6 Hz), 1.05 (3H, d, J = 6.4 Hz), 1.06 (3H, d, J = 6.7 Hz), and 1.18 (3H, d, J = 6.1 Hz); two vinyl methyls at δ 1.55 (3H, s) and 1.56 (3H, s); and two methyl singlets at δ 1.30 (3H, s) and 1.35 (3H, s). Additionally, the ^{1}H NMR spectrum showed signals corresponding to two methoxyl groups at δ 3.29 (3H s) and 3.36 (3H, s) and to numerous oxymethine and olefinic protons resonating between δ 3.25–4.05 and δ 5.35–7.35, respectively. Analysis of the ^{13}C NMR assignments, made primarily from the ^{1}H−^{13}C HSQC spectra, revealed the somewhat surprising presence of 16 olefinic methine carbons, two olefinic quaternary carbons, 16 oxymethine carbons, and six carbonyls (see Table 1). Together these data suggested a polyketide-type structure for **1**.

A detailed analysis of the homonuclear and heteronuclear 2D NMR data allowed us to identify three main fragments (A−C, Figure 1) along with a β-hydroxyaspartic acid (β-OHAsp) residue. The constitution of the largest fragment (A) was deduced as follows. A conjugated pentaene spin system ($\delta_{H\text{-}5}$ 6.22, $\delta_{C\text{-}5}$ 123.7, $\delta_{H\text{-}6}$ 7.35, $\delta_{C\text{-}6}$ 143.1, $\delta_{H\text{-}7}$ 6.51, $\delta_{C\text{-}7}$ 131.0, $\delta_{H\text{-}8}$ 6.78, $\delta_{C\text{-}8}$ 142.0, $\delta_{H\text{-}9}$ 6.51, $\delta_{C\text{-}9}$ 133.9, $\delta_{H\text{-}10}$ 6.65, $\delta_{C\text{-}10}$ 138.7, $\delta_{H\text{-}11}$ 6.52, $\delta_{C\text{-}11}$ 134.0, $\delta_{H\text{-}12}$ 6.53, $\delta_{C\text{-}12}$ 135.7, $\delta_{H\text{-}13}$ 6.54, $\delta_{C\text{-}13}$ 136.2, $\delta_{H\text{-}14}$ 5.68, $\delta_{C\text{-}14}$ 134.8) assigned from HOHAHA, COSY, HSQC, and HMBC correlations was linked to a carbonyl group by HMBC correlations from the H-5 and H-6 protons to the carbon resonance at δ 169.0 (C-4). COSY, HSQC-HOHAHA, and HMBC correlations extended this pentaene system by an additional oxymethine ($\delta_{H\text{-}15}$ 4.03, $\delta_{C\text{-}15}$ 80.7), and HMBC correlations from H-15 to C-16 and C-17 and ROESY correlations between H-15 and H-18 and H-20 connected this fragment in turn to a tetrasubstituted tetrahydropyran ring. In similar fashion, uninterrupted conectivities from the tetrahydropyran's oxymethine at δ 3.65 (H-20) to the oxymethine proton at δ 3.55 (H-24) and from the olefinic proton at δ 4.91 (H-26) through to Me-67 at δ 1.18 were established from the same set of 2D NMR spectra. Finally, long-range correlations from the methyl olefinic

† Dedicated to Dr. G. Robert Pettit of Arizona State University for his pioneering work on bioactive natural products.

* To whom correspondence should be addressed. Tel: (301) 594-5187. Fax: (301) 402-0008. E-mail: caroleb@mail.nih.gov.

10.1021/np070603p CCC: $40.75
Published on Web 02/14/2008

Table 1. NMR Spectroscopic Data for Compound **1** (600 MHz, CD_3OD)

	δ_C	δ_H (J in Hz)	HMBC[a]	ROESY[b]
1	172.7			
2	55.9	5.16 br s	1, 4, 35	
3-NH				
4	169.0			
5	123.7	6.22 d (14.9)	4, 6 7	7
6	143.1	7.35 dd (14.9, 11.3)	4, 7, 8	8
7	131.0	6.51 m	5, 8	5
8	142.0	6.78 dd (14.7, 11.3)	6, 10	6, 10
9	133.9	6.51 m	8, 10, 11	26
10	138.7	6.65 dd (14.2, 9.7)	8, 12	8
11	134.0	6.52 m	9	24
12	135.7	6.53 m	10, 13	14, 24, OMe-79
13	136.2	6.54 m	12	15
14	134.8	5.68 dd (14.8, 9.5)	12	12, 16
15	80.7	4.03 t (9.5)	13, 16, 17, OMe-79	13, 14, 18, 20, OMe-79
16	79.2	3.81 dd (9.5, 2.0)	15, 17, 18, 20	14, 17, 19a, OMe-37, OMe-79
17	78.8	3.27 br d (2.0)	OMe-37, 18, 19	16, 18
18	31.8	2.06 m		15, 17, 19a, Me-38
19a	35.4	1.36 m	20	16
19b		1.25 m	20	20
20	69.8	3.65 m	16	13, 15, 18
21a	42.9	1.41 m	20	
		1.23 m	20	
22	66.5	4.02 m	21, Me-39	13, 14, 23, 24, 26
23	42.5	1.35 m	Me-39	22
24	80.9	3.55 d (9.7)	22, 23, 26, Me-40	13, 22, 26, Me-39
25	137.3			
26	134.7	4.91 s	24, Me-40, Me-41	22, 24, 27, Me-41
27	38.9	2.32 m	28	29, Me-40
28	79.2	3.49 t (8.6)	26, 27, 30, Me-41	26, 27, 29, 30
29	134.0	5.37 dd (15.8, 8.6)	30, 31	27, 31b, Me-41
30	132.9	5.50 m	28	28, 32
31a	42.0	2.13 m		29, 30
31b		2.08 m	32	29, 32
32	67.3	3.29 m		29, 4
33a	41.1	1.76 m	34	42
33b		1.57 m	32	34, 42
34	73.5	5.51 m	1	32, 33a, 42
35	71.4	4.88 br s	2, 36	
36	172.7			
OMe-37	57.5	3.36 s	17	16, Me-38
Me-38	15.8	1.05 d (6.4)	17, 18, 19	17, OMe-37
Me-39	8.6	0.54 d (7.0)	22, 23, 24	23, 24
Me-40	10.5	1.56 s	24, 25, 26	27
Me-41	17.9	0.68 d (6.7)	26, 27, 28	26, 27, 28, 29
42	58.1	3.93 m	33, 44, 66, 67	33b, 34, Me-67
43-NH				
44	174.8			
45	44.9	2.45 d (6.4)	44, 46, 47	46
46	69.6	3.96 m		45, 47a
47a	35.7	1.62 m		46
47b		1.51 m		46
48	30.1	1.34 m		
49	36.4	1.67 m		50
50	84.0	3.703 d (8.0)	49, 52, Me-68	48, 55
51	137.7			
52	130.4	5.45 d (10.2)	50, Me-69	50, 55
53	35.7	2.71 m	51	54, Me-69
54	75.9	3.70 dd (8.0, 3.6)	55, 71, Me-70	52, 53, Me-70
55	53.2	4.14 br d (8.0)	54	52, 53, 71, Me-74
56-NH				
57	167.4			
58	123.8	6.23 d (15.6)	57, 60	Me-75, Me-76
59	148.6	6.99 d (15.6)	57, 58, 60, 75, 76	62, Me-75, Me-76
60	52.0			
61	217.2			
62	45.6	3.17 dq (9.8, 6.9)	61, 63, Me-77	59, 64, Me-76, Me-78
63	78.3	3.60 dd (9.8, 2.8)	61, 62, 65, Me-78	64, Me-65, Me-77
64	29.8	1.80 m	Me-65, Me-78	63, Me-65, Me-78
Me-65	20.4	0.988 d (6.9)	63, 64, Me-78	
66	67.8	3.91 m	Me-67	34, Me-67
Me-67	20.9	1.18 d (6.1)	42, 66	34, 42
Me-68	15.6	0.99 d (6.5)	48, 49, 50	49, 50
Me-69	11.9	1.55 s	50, 51, 52	53
Me-70	17.9	1.06 d (6.7)	52, 53, 54	52, 53, 54, 55

Table 1. Continued

	δ_C	δ_H (J in Hz)	HMBC[a]	ROESY[b]
71	76.3	3.63 br d (9.0)	72, Me-75, Me-76	53, 55, Me-73, Me-74
72	31.8	1.54 m		
Me-73	20.0	1.02 d (6.6)	71, 72, Me-74	71, 72
Me-74	19.5	0.95 d (6.6)	71, 72, Me-73	55, 72
Me-75	23.8	1.30 s	59, 60, 61, Me-76	59, 62
Me-76	23.8	1.35 s	59, 60, 61, Me-75	59, 62
Me-77	15.8	0.92 d (6.8)	61, 62, 63	62, 63, 64
Me-78	14.1	0.87 d (6.9)	63, 64, 65	62, 64
OMe-79	56.3	3.29 s	17	12, 14, 15

[a] Proton showing HMBC correlation to indicated carbon. [b] Proton showing ROESY correlation to indicated proton.

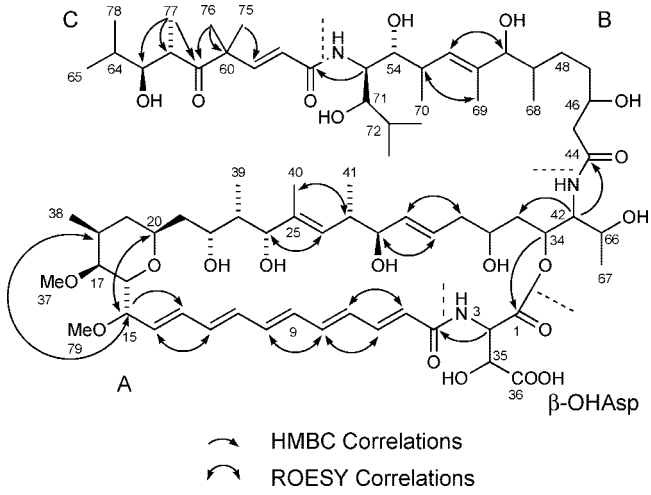

Figure 1. NMR- and MS-based connectivity of the fragments of mirabilin. Fragments A−C and the β-hydroxyaspartic acid (β-OHAsp) unit are indicated by dashed lines. Key HMBC correlations used to connect the fragments of **1** and ROESY correlations used to establish the configuration of the double bonds and tetrahydropyran ring are indicated by single- and double-sided arrows, respectively.

protons at δ 1.56 (Me-40) to the carbon resonances at δ 80.9 (C-24), 137.3 (C-25), and 134.7 (C-26) connected these two spin systems and assembled the structure of fragment A.

Two spin systems in fragment B comprising C-45 to C-50 and C-52 to C-55, which includes the side chain C-71 to C74, were readily apparent, and HMBC correlations from the vinyl methyl at δ 1.55 (Me-69) to the carbon resonances at δ 84.0 (C-50), 137.7 (C-51), and 130.4 (C-52) connected the two. The complete structure of fragment B was obtained from additional HMBC correlations between the methylene protons at δ 2.45 (H-45) and the amide carbonyl at δ 174.8 (C-44). The composition of fragment C was revealed from key HMBC correlations including those from the methyl protons at δ 0.92 (Me-77), 1.30 (Me-75), and 1.35 (Me-76) to the ketone carbon at δ 217.2 (C-61); from the methyl protons Me-75 and Me-76 to the carbon resonances at δ 52.0 (C-60) and 148.6 (C-59); and from the olefinic protons at δ 6.23 (H-58) and 6.99 (H-59) to the carbonyl carbon at δ 167.4 (C-57). The last remaining spin system was assigned to β-OHAsp from the NMR data. The oxymethine proton at δ 5.51 (H-34) appearing relatively downfield was indicative of a carboxylic acid ester at this position and was confirmed by an HMBC correlation from H-34 to the α-carbonyl carbon of β-OHAsp at δ 172.3 (C-1). This linkage thus established the presence of a 35-membered macrolide lactam ring in **1**. Finally, the complete structure of **1** was established from the HMBC spectra. A long-range correlation from the proton signal at δ 3.93 (H-42) to the carbonyl carbon at δ 174.8 (C-44) linked fragment B to the macrolide ring, while an HMBC correlation between the proton signal at δ 4.14 (H-55) to the carbon resonance at 167.4 (C-57) established the connectivity between fragments B and C. In addition to these HMBC correlations, dipolar correlations of the amide protons were used to corroborate these results. The ROESY spectrum of **1** acquired in DMF-d_7 (see Table S1 for complete ^{1}H and ^{13}C NMR assignments) showed ROEs from NH-3 (δ 8.08) to the olefinic proton H-5 (δ 6.40) and the α-proton of β-OHAsp (δ 5.16), confirming the linkage of β-OHAsp to fragment A. Connectivity between fragment B and the macrolide ring (fragment A) was confirmed from ROEs from the amide proton NH-43 (δ 7.63) to H-45 (δ 2.44) and H-34 (δ 5.50), while connectivity between fragments B and C was deduced from ROE correlations between the amide proton NH-56 (δ 7.60) and H-55 (δ 4.11) and H-58 (δ 6.39).

Tandem mass spectrometry provided further evidence to support the structure of **1**. The negative ESIMS/MS spectrum of the major ion peak at m/z 1428 displayed an intense ion at m/z 1410 [M − H − H_2O]$^-$. MS of the daughter ion peak displayed fragment ions at m/z 1366 [M − H − H_2O − -44]$^-$ due to the loss of CO_2 (presumably due to decarboxylation of βOH-Asp) and m/z 828 [M − H − H_2O − 583]$^-$ corresponding to the loss of fragments B and C. Finally, MS^4 experiments of the ion peak at m/z 1366 produced a fragment ion at m/z 1141 [M − H − H_2O − 44 – 225]$^-$ corresponding to the loss of fragment C (see Figure 1). Thus, the MS/MS, MS^3, and MS^4 fragmentation patterns were in complete agreement with the structure of **1** determined by NMR.

On the basis of the structural features of **1**, it was evident that mirabilin is a new member of the chondropsin family of macrolide lactams that currently comprise chondropsins A−D, 73-deoxychondropsin A, and poecillastrins A−C. Chondropsins and poecillastrins are potent cancer cell growth inhibitors that have 35-membered macrolide lactam rings, with the exception of chondropsin D and poecillastrin A, which contain 37-membered and 33-membered macrolactam rings, respectively.[7a−f] To date, these macrolides have come from collections of the marine sponges *Chondropsin* sp. (chondropsins A, B, and D),[7a,b] *Ircinia ramosa* and *Ircinia* sp. (chondropsin C and 73-deoxychondropsin A),[7c] *Psammoclemma* sp. (chondropsin A and 73-deoxychondropsin A),[7d] and *Poecillastra* sp. (poecillastrins A−C).[7e,f]

Neither total synthesis nor complete determination of the absolute stereochemistry of any of the chondropsin-like macrolides has been reported. Likewise, due to the large number of chiral centers and complexity of mirabilin, together with the small amount of material obtained, we were unable to fully assign the relative configuration of **1**. However, by the combined analysis of $^3J_{H-H}$ coupling constants and ROESY spectra, we were able to establish the geometry for each of the double bonds and the relative configuration for most of the chiral centers as follows. The ^{1}H NMR spectra and a phase-sensitive ^{1}H,^{13}C-HSQC spectrum[8] optimized to show ^{1}H−^{1}H coupling constants in the acquisition dimension revealed large $^3J_{H-H}$ values (14–15 Hz, Table 1) for the C5−C6, C7−C8, C9−C10, C11−C12, C13−C14, C29−C30, and C58−C59 double bonds, indicating E configurations for each. The C25−C26 double bond was assigned an E configuration on the basis of ROEs between vinylic methyl group Me-40 and H-27, and olefinic protons H-26 and H-24. Similarly, the C51−C52 double bond was assigned an E configuration from ROEs between vinylic methyl group Me-69

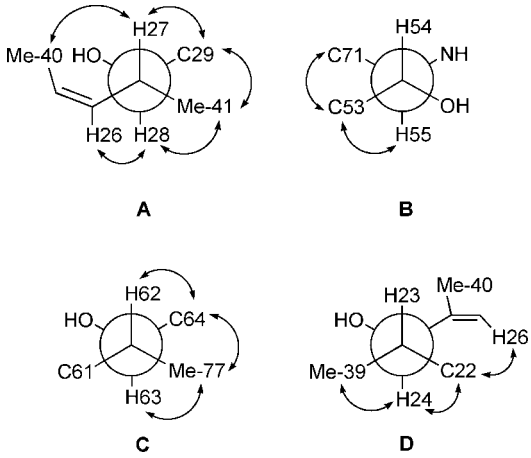

Figure 2. Newman projections and ROESY correlations used to establish the relative configurations of (A) C-27/C-28, (B) C-54/C-55, (C) C-62/C-63, and (D) C-23/C-24.

and H-53, and olefinic protons H-52 and H-50. A small $^3J_{H16-H17}$ of 2.0 Hz obtained from a phase-sensitive COSY-35 spectrum[9] indicated an equatorial orientation for H-16 in the tetrahydropyran ring, and strong ROEs from H-15 to H-18 and H-20 indicated an axial orientation for H-18 and H-20. Finally, another small $^3J_{H17-H18}$ of 4.9 Hz in the COSY-35 spectrum showed H-17 to be equatorial, to give the relative configuration of the tetrahydropyran ring shown in Figure 1. Interestingly, transannular ROEs were observed between H-13 and H-24 and between the proton signal at δ 6.52 (corresponding to either H-11 or H-9) and H-24 and H-26, consistent with the relative configurations shown in Figure 1.

The relative configurations of stereogenic centers at C-23/C-24, C-27/C-28, C-54/C-55, and C-63/C-64 were established by analyzing their homonuclear coupling constants and ROESY correlations and comparing these data to those predicted for all possible staggered rotamers (Figure 2).[10] The *anti* configuration between Me-41 and the hydroxyl group at C-28 was apparent from the large coupling constant between H-27 and H-28 (8.6 Hz) and an ROE between Me-41 and H-29, and the coupling constant between H-54 and H-55 (8.0 Hz) and an ROE between H-53 and H-71 indicated a *syn* configuration at C-54/C-55 (Figure 2b), while the *anti* configuration between Me-77 and the C-63 hydroxyl group was assigned from the large coupling constant between H-62 and H-63 (9.8 Hz), together with ROESY correlations between H-62 and H-64, H-64 and Me-77, and Me-77 and H-63 (Figure 2c). A large $^3J_{H23-H24}$ value of 9.7 Hz showed H-23 and H-24 to be *anti*, and ROEs between H-22 and H-24, H-24 and Me-39, and H-22 and H-26 established a *syn* relationship between Me-39 and the hydroxyl group at C-24 (Figure 2d). Finally, the relative configuration at C-22/C-23 was solved by using Kishi's universal NMR database: Comparison of the carbon chemical shift of Me-39 (δ 8.6) with those reported for all possible diastereomers of 2-methyl-1,3-diol indicated a *syn*/*syn* configuration for C-22/C-23/C-24.[11] This result is in agreement with the C-23/C-24 configuration established above using Murata's approach. We note that although the relative stereochemistries for the spin systems above have been indicated in the chemical structures of **1**, they do not interrelate between each other and their boundaries correspond to the projections shown in Figure 2.

Mirabilin was unstable to ambient light and degraded within 3–4 h. While 1D and 2D NMR spectra of the degradation product contained signals that clearly corresponded to the polyketide side chain (fragments B and C, Figure 1), signals corresponding to the macrocyclic ring were absent (see Supporting Information). We suspect that photodegradation of the highly conjugated polyene resulted in polymerization or destruction of the 35-membered lactam ring.

Mirabilin is a potent inhibitor of tumor cell proliferation *in vitro*, inhibiting the growth of the tumor cell line HCT-116 with an IC_{50} value of 0.27 $\pm$ 0.09 μM. Moreover, mirabilin did not inhibit the growth of monkey kidney nor human cervical carcinoma cell lines at concentrations as high as 70 μM. The degradation product of mirabilin, which comprises the linear polyketide comprising fragments B and C, did not inhibit growth of tumor cells at concentrations as high as 100 μg/mL. Thus, the macrolide lactam ring is essential to mirabilin's antitumor activity, and the polyketide side chain alone cannot inhibit tumor cell growth. Unlike some polyene macrolides, mirabilin did not inhibit the growth of *Candida albicans*.

In summary, mirabilin is a new chondropsin-type macrolide characterized by the presence of a 35-membered lactam ring, where the macrolactam ring contains a fully conjugated pentadiene system along with a tetrasubstituted tetrahydropyran ring. A linear polyketide chain extends from the macrocyclic ring through an amide linkage. Mirabilin represents the first example of a macrolide of the chondropsin family to possess a conjugated pentadiene and a tetrasubstitued tetrahydropyran ring. As expected for macrolides of this type, mirabilin exhibited potent cytotoxicity toward a human colon tumor cell line. Finally, although chondropsins and poecillastrins have been isolated from four taxonomically diverse sponges,[7a–f] mirabilin is the first example of a chrondopsin-type macrolide to be isolated from a member of the Theonellidae family.

Experimental Section

General Experimental Procedures. Optical rotations were measured with a Perkin-Elmer 341 polarimeter, and UV spectra were recorded on an Agilent 8453 spectrophotometer. NMR spectra were recorded in CD_3OD on a Bruker DRX-600 spectrometer (^{1}H at 600 MHz, ^{13}C at 125 MHz) using the residual solvent signal as an internal reference. Standard pulse sequences were employed for DQF-COSY, 2D-HOHAHA, HSQC, HMBC, and ROESY experiments. Phase-sensitive ROESY spectra with water suppression were recorded using a mixing time of 400, 300, and 250 ms; HSQC experiments were optimized for $^1J_{C-H}$ = 145 Hz, and HMBC spectra were optimized for $^{2,3}J_{C-H}$ = 10, 8, and 5 Hz. The accurate mass electrospray ionization (ESI) mass spectra were measured on a Waters LCT Premier time-of-flight (TOF) mass spectrometer. The instrument was operated in Ω-mode at a nominal resolution of 10 000. The electrospray capillary voltage was set at 2 kV and the sample cone voltage at 60 V. The desolvation temperature was set to 275 °C, and nitrogen was used as the desolvation gas with a flow rate of 300 L/h. Accurate masses were obtained using the internal reference standard method. The sample was introduced into the mass spectrometer via the direct loop injection method. Both positive and negative ion accurate mass data were achieved by reversing the instrument's operating polarity. LCMS analyses were carried out using an Agilent 1100 MSD integrated LCMS system employing negative ion ESI mode.

Biological Material. Samples of *Siliquariaspongia mirabilis* (de Laubenfels, 1954) (lithistid Demospongiae: family Theonellidae) were collected southeast of Chuuk lagoon in the Federated States of Micronesia at a depth of 50 m in 1994. The sample was identified as described previously,[6] and a voucher specimen has been deposited at the Natural History Museum, London, United Kingdom (BMNH 2007.7.9.1).

Extraction and Isolation. Samples were frozen immediately after collection and shipped on dry ice to Frederick, MD, where they were freeze-dried and extracted with H_2O (OCDN 2547). A 6 g portion of the aqueous extract was partitioned with *n*-BuOH−H_2O (1:1) to afford a dried *n*-BuOH extract (0.7 g), which was fractionated on a Sephadex LH-20 column (50 × 2.5 cm) equilibrated and eluted with MeOH. Fractions containing mirabilin were combined and the solvent was removed *in vacuo* to give 148 mg of a yellow film, which was subsequently purified by reversed-phase HPLC (Synergi Fusion C18, 250 × 10 mm, 4 μm, DAD at 330 nm) eluting with a linear gradient of 50–80% MeOH in 0.05% TFA in 50 min to afford compound **1** (1.5 mg, t_R = 30.2 min).

Mirabalin (1): pale yellow, amorphous powder; $[\alpha]^{25}_D$ −14 (*c* 0.05, MeOH); IR ν_{max} 3380, 1680, 1650, 1207 cm^{-1}; UV (MeOH) λ_{max} (log

ϵ) 350 (3.96) nm; ^{1}H and ^{13}C NMR data, see Table 1; HRESIMS *m/z* 1428.8442 [M − H]$^-$, (calcd for $C_{76}H_{122}N_3O_{22}$, 1428.8520).

Biological Assays. Cytotoxicity assays were carried out using an MTT cell proliferation assay (American Type Culture Collection) according to manufacturer's instructions. Briefly, HCT-116 (human colon carcinoma cell line), B-SC1 (monkey kidney cell line), or HeLa (human cervical carcinoma cell line) cells were seeded in 96-well tissue culture plates at a density of 2×10^4 cells/well in 50 μL of growth media and allowed to adhere for 18 h. Attached cells were incubated with extracts, fractions, pure mirabilin, or solvent (as a negative control) for 24 h before replacing the growth media with fresh media. Following an additional 72 h incubation, cell viability was assessed upon treatment with MTT (A_{570}, Molecular Devices 96-well absorbance plate reader).

Acknowledgment. We thank the Coral Reef Research Foundation, D. Newman, and the state of Chuuk, Federated States of Micronesia, for facilitating sample acquisition; M. Kelly for taxonomy;[6] E. Gustchina for assistance with biological assays; and J. Lloyd for HRMS data. This work was supported in part by the NIH Intramural Research Program (NIDDK) and the Intramural AIDS Targeted Antiviral Program, Office of the Director, NIH (C.A.B.).

Supporting Information Available: ^{1}H and ^{13}C NMR data for **1** in DMF-d_7; 1D ^{1}H, HSQC, HMBC, 2D-HOHAHA, DQF-COSY, and ROESY spectra for **1** in CD_3OD; 1D ^{1}H NMR spectrum of degradation product; and ESIMS-MS spectra. This material is available free of charge via the Internet at http://pubs.acs.org.

References and Notes

(1) Bewley, C. A.; Faulkner, D. J. *Angew. Chem., Int. Ed.* **1998**, *37*, 2162–2178.

(2) (a) Kashman, Y.; Carmely, S. *Tetrahedron Lett.* **1985**, *26*, 511–514. (b) Kobayashi, M.; Tanaka, J.; Katori, T.; Matsuura, M.; Kitagawa, I. *Tetrahedron Lett.* **1989**, *22*, 2963–2966. (c) Kitagawa, I.; Kobayashi, M.; Katori, T.; Yamashita, M.; Tanaka, J.; Doi, M.; Ishida, T. *J. Am. Chem. Soc.* **1990**, *112*, 3710–3712. (d) Kobayashi, M.; Tanaka, J.; Katori, T.; Matsuura, M.; Yamashita, M.; Kitagawa, I. *Chem. Pharm. Bull.* **1990**, *38*, 2409–2418. (e) Doi, M.; Ishida, T.; Kobayashi, M.; Kitagawa, I. *J. Org. Chem.* **1991**, *56*, 3629–3632. (f) Tsukamoto, S.; Ishibashi, M.; Sasaki, T.; Kobayashi, J. *J. Chem. Soc., Perkin Trans. 1* **1991**, *3185*, 3188. (g) Youssef, D. T. A.; Mooberry, S. L. *J. Nat. Prod.* **2006**, *69*, 154–157.

(3) (a) Sakai, R.; Higa, T.; Kashman, Y. *Chem. Lett.* **1986**, *1499*, 1502. (b) Kato, Y.; Fusetani, N.; Matsunaga, S.; Hashimoto, K.; Sakai, R.; Higa, T.; Kashman, Y. *Tetrahedron Lett.* **1987**, *28*, 6225–6228.

(4) (a) D'Auria, M. V.; Gomez Paloma, L.; Minale, L.; Zampella, A.; Verbist, J. F.; Roussakis, C.; Debitus, C. *Tetrahedron* **1993**, *49*, 8657–8664. (b) D'Auria, M. V.; Gomez Paloma, L.; Minale, L.; Zampella, A.; Verbist, J. F.; Roussakis, C.; Debitus, C. *Tetrahedron* **1994**, *50*, 4829–4834.

(5) (a) D'Auria, M. V.; Gomez Paloma, L.; Minale, L.; Zampella, A.; Debitus, C. *J. Am. Chem. Soc.* **1994**, *116*, 6658–6663. (b) D'Auria, M. V.; Debitus, C.; Paloma, L. G.; Minale, L.; Zampella, A. *J. Nat. Prod.* **1994**, *57*, 1595–1597.

(6) Plaza, A.; Gustchina, E.; Baker, H. L.; Kelly, M.; Bewley, C. A. *J. Nat. Prod.* **2007**, *70*, 1753–1760.

(7) (a) Cantrell, C. C.; Gustafson, K. R.; Cecere, M. R.; Pannell, L. K.; Boyd, M. R. *J. Am. Chem. Soc.* **2000**, *122*, 8825–8829. (b) Rashid, M. A.; Cantrell, C. L.; Gustafson, K. R.; Boyd, M. R. *J. Nat. Prod.* **2001**, *64*, 1341–1344. (c) Rashid, M. A.; Gustafson, K. R.; Boyd, M. R. *Tetrahedron Lett.* **2001**, *42*, 1623–1626. (d) Chevallier, C.; Laprevote, O.; Bignon, J.; Debitus, C.; Guenard, D.; Sevenet, T. *Nat. Prod. Res.* **2004**, *18*, 479–484. (e) Rashid, M. A.; Gustafson, K. R.; Crouch, R. C.; Groweiss, A.; Pannell, L. K.; Van, Q. N.; Boyd, M. R. *Org. Lett.* **2002**, *4*, 3293–3296. (f) Takada, K.; Choi, B. W.; Rashid, M. A.; Gamble, W. R.; Cardellina, J. H., II; Van, Q. N.; Lloyd, J. R.; McMahon, J. B.; Gustafson, K. R. *J. Nat. Prod.* **2007**, *70*, 428–431.

(8) Schleucher, J.; Schwendinger, M.; Sattler, M.; Scmidt, P.; Schedletzky, O.; Glaser, S. J.; Sorensen, O. W.; Griesinger, C. *J. Biomol. NMR* **1994**, *4*, 301–306.

(9) Bax, A.; Freeman, R. *J. Magn. Reson.* **1981**, *44*, 542–561.

(10) Matsumori, N.; Kaneno, D.; Murata, M.; Nakamura, H.; Tachibana, K. *J. Org. Chem.* **1999**, *64*, 866–876.

(11) (a) Kobayashi, Y.; Tan, C. H.; Kishi, Y. *J. Am. Chem. Soc.* **2001**, *123*, 2076. (b) Bifulco, G.; Dambruoso, P.; Gomez-Paloma, L.; Riccio, R. *Chem. Rev.* **2007**, *107*, 3744–3779.

NP070603P